

Reversible Control of Spacing in Charged Lamellar Membrane Hydrogels by Hydrophobically Mediated Tethering with Symmetric and Asymmetric Double-End-Anchored Poly(ethylene glycol)s

Chenyu Liu^{1,3§}, Kai K. Ewert^{1§}, Emily Wonder¹, Phillip Kohl^{1,2}, Youli Li^{1,2}, Weihong Qiao^{3*}, Cyrus R. Safinya^{1*}

¹ Materials, Physics, and Molecular, Cellular & Developmental Biology Departments, University of California at Santa Barbara, Santa Barbara, California 93106

² Materials Research Laboratory, University of California at Santa Barbara, Santa Barbara, California 93106

³ State Key Laboratory of Fine Chemicals, School of Chemical Engineering, Dalian University of Technology, Dalian, 116024, P. R. China

§These authors contributed equally

*Corresponding authors contact information: safinya@mrl.ucsb.edu, qiaowei hong@dlut.edu.cn

Key words

PEG-lipid, lamellar phase, lipid bilayer, lipid membrane, hydrophobic mediated tethering, self-assembly

Abstract

Complex materials often achieve their remarkable functional properties by hierarchical assembly of building blocks via competing and/or synergistic interactions. Here, we describe the properties of new double-end-anchored poly (ethylene glycol)s (DEA-PEGs), macromolecules designed to impart hydrophobically mediated tethering attractions between charged lipid membranes. We synthesized DEA-PEGs (MW 2000 (2K) and 4.6K) with two double-tail (symmetric) or a double-tail and a single-tail (asymmetric) hydrophobic end anchors and characterized their equilibrium and kinetic properties using small-angle X-ray scattering. Control multilayer membranes without and with PEG-lipid (i.e. single-end-anchored PEG) swelled continuously with the interlayer spacing increasing between 30wt% and 90wt% water content, due to electrostatic as well as, in the case of PEG-lipid, steric repulsion. In contrast, interlayer spacings in lamellar membrane hydrogels containing DEA-PEGs expanded over a limited water dilution range and reached a “locked” state, which displayed a near constant membrane wall-to-wall spacing (δ_w) with further increases in water content. Remarkably, the locked state displays a simple relation to the PEG radius of gyration $\delta_w \approx 1.6 R_G$ for both 2K and 4.6K PEG.

Nevertheless, δ_w being considerably less than the physical size of PEG ($2(5/3)^{1/2}R_G$) is highly unexpected and implies that, compared to free PEG, anchoring of the PEG tether at both ends leads to a considerable distortion of the PEG conformation confined between layers. Significantly, the lamellar hydrogel may be designed to *reversibly* transition from a locked to an unlocked (membrane unbinding) state by variations in the DEA-PEG concentration controlling the strength of the interlayer attractions due to bridging conformations. The findings with DEA-PEGs have broad implications for hydrophobic-mediated assembly of lipid- or surfactant- coated building blocks with distinct shape and size, at predictable spacing, in aqueous environments.

Introduction

Complex natural materials, including surfaces, often achieve their remarkable properties by a hierarchical assembly of building blocks via orthogonal competing interactions.¹⁻⁷ Inspired by this, we sought to harness hydrophobic interactions for mediating the assembly of building blocks beyond the simple self-association of amphiphilic molecules or moieties. To this end, we designed double-end-anchored poly(ethylene glycol)s (DEA-PEGs), i.e., hydrophilic PEG polymer modified with hydrophobic groups on both ends, that can be broadly used to control interactions between amphiphilic assemblies (e.g. lipid membranes) (Figure 1A).

PEG is a highly biocompatible polymer that, when anchored to a surface, is capable of shielding the surface by steric repulsion.^{8,9} This has been exploited for imparting or increasing the stability of colloids, in particular in the presence of salt. (The presence of salt renders stabilization based on charge ineffective.) PEG is further used to increase the circulation time of liposomes *in vivo* in drug delivery applications by the addition of PEG-lipids (i.e. single-end-anchored PEG, SEA-PEG) to create so-called STEALTH liposomes (spherical lipid bilayer membranes with protruding polymers in the brush conformation designed to repel immune cell surfaces).¹⁰⁻¹⁶ In this application, the typical molecular weight of PEG used is 2000 or 5000 g/mol. In addition to thus imparting repulsive interactions, PEG-lipids have been used to mediate specific attractive interactions by attaching a targeting ligand at the distal (to the lipid) end of the PEG chain.¹⁷⁻²⁴

DEA-PEGs bear two hydrophilic groups at opposing ends of the PEG chain, which means that they may assume either a looping or a bridging conformation (Figure 1B). These conformations can interconvert via a transitional state with one of the hydrophobic groups inside the water phase (Figure 1B, right). While DEA-PEGs in the looping conformation behave similarly to simple PEG-lipids, the bridging conformation gives rise to an attractive interaction²⁵⁻²⁷ and therefore has the potential to greatly affect the behavior of the lamellar phase. Intriguingly, the bridging conformations of double-end-anchored polymer surfactants have also been shown to destabilize hydrogels of lipid membranes, in the case of hydrogels stabilized by defects.²⁷⁻³²

Hydrogels are three-dimensional, hydrophilic, often polymeric networks capable of absorbing large amounts of water or biological fluids. Due to their high water content, hydrogels compose an important class of soft materials from both a technological and a scientific point of view.³³ Their diverse applications range from contact lenses and wound dressings to drug delivery systems, tissue engineering substrates, and hygiene products.³⁴⁻⁴⁶ Typical parameters that control the properties of hydrogels are the chemical nature of the network, the density of crosslinks, and the affinity to water.

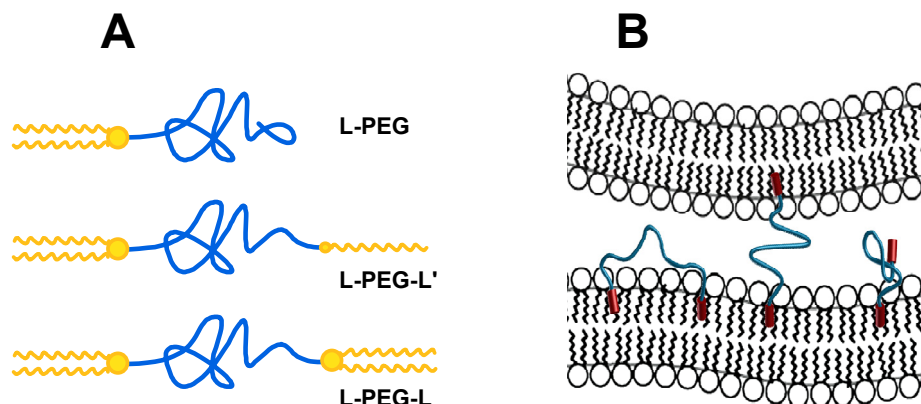


Figure 1. Design of single and double-ended PEG lipids and control of inter-membrane interaction by tethering. (A) Schematic depictions of the single and double-end-anchored PEG-lipids used in this study. (B) Schematic depiction of the possible conformations of double-end-anchored PEG-lipids in opposing lipid bilayer membranes. The looping (left) and bridging (center) conformations can interchange through the intermediate state with one anchor in the aqueous layer (right, related to the barrier between conformations). The cross-bridging conformation fixes opposing membranes in close proximity in the presence of excess water.

We explored several means of tuning the interactions between lipid bilayer membranes mediated by the DEA-PEGs. Variation of the length of the PEG chain allows control of the range of the interactions. Changing one end from a double-tail- to a single-tail-anchor should increase the probability for the transitional state between the bridging and looping conformations (Figure 1B, right); thus, suppressing the barrier for interconversion of the two conformations. The rationale for this expectation is that single-tail surfactants have a critical micelle concentration that is several orders of magnitude higher than that of double-tail lipids. Nature exploits this ability of single-tail lipids to readily leave the membrane by using lysolipids as signaling molecules.⁴⁷ We thus synthesized a series of DEA-PEGs by functionalizing PEG with either two dioleoyl lipid groups (i.e. symmetric DEA-PEGs, labeled L-PEG-L, bottom cartoon in Fig. 1A) or one dioleoyl and one oleoyl group (asymmetric DEA-PEGs, labeled L-PEG-L',

middle cartoon in Fig. 1A). We also synthesized corresponding single-end-anchored PEGs (dioleoyl tail, L-PEG, top cartoon in Fig. 1A) as a control compound.

Using small-angle X-ray scattering (SAXS) we studied the effect of adding the DEA-PEGs, for both 2K PEG and 4.6K PEG, on the forces between charged membranes in a lamellar phase, by varying the water content between 30 wt% and 90 wt%. The membranes consisted of an approximately equimolar mixture of 1,2-dioleoyl-*sn*-glycerol-3-phosphatidyl-choline (DOPC) and *N*-[1-(2,3-dioleoyloxy)propyl]-*N,N,N*-trimethylammonium methyl-sulfate (DOTAP). The DEA-PEGs and PEG-lipid controls were incorporated into the bilayer at a low concentration, to minimize the lateral interactions of neighboring PEG chains and prevent lateral phase separation in the plane of the membrane. We found that the bridging conformations of DEA-PEGs control the extent of swelling of the lamellar phase in a manner depending on the PEG MW (or equivalently the PEG length), while the strength of the attractive interaction conferred by the bridging conformation was dependent on the DEA-PEG concentration. Furthermore, the structure of the anchoring group was found to have a strong influence on the kinetics: the asymmetric DEA-PEGs reached equilibrium faster, likely because their one single-tail anchor enables faster interchange between the bridging and looping conformations.

At 5 mol% DEA-PEGs the membrane wall-to-wall spacing (δ_w) of the lamellar hydrogel was maintained in a locked state with very small variations in the water layer spacing between 60 wt% to 80 wt% for PEG2K and 70 wt% and 90 wt% for PEG4.6K. The locked state is a direct indication of interlayer attractions from bridging dominating looping conformations of DEA-PEGs. Notably, the constant water spacing, which is set by the radius of gyration (R_G) of the PEG tether followed a very simple relation, $\delta_w \approx 1.6 R_G$, for both PEG MWs. However, the finding that δ_w in the locked state is significantly less than the physical size of the PEG tether ($= 2R_{\text{physical}} = 2(5/3)^{1/2}R_G$) is unexpected and implies that end-anchored PEG between the layers is considerably more compressed compared to free PEG. While the locked state is stable for the PEG4.6K tether as the strength of the bridging interaction is decreased by lowering the concentration of DEA-PEGs from 5 mol% to 2.5 mol%, a notably different behavior is found for the smaller PEG2K tether where lowering the concentration of DEA-PEGs to 2.5 mol% results in the locked state between 60 wt% and ≈ 75 wt% water followed by a *reversible* unbinding of the membranes between 75 wt% and 80 wt% water.

The results of the work described here with DEA-PEGs are expected to have far reaching implications in science and nanotechnology and open a new direction for *hydrophobic-mediated* assembly of objects with distinct shape and size, at predictable spacing, in aqueous environments. The objects may include spherical, rod-like, and discoidal vesicles and micelles, and a range of hybrid lipid- or surfactant-coated organic and inorganic nanomaterials. This is a promising but under-explored strategy in contrast to current prevalent approaches to directed assembly of water-soluble building blocks where nonspecific electrostatic interactions (e.g.,

between intrinsically disordered protein polyampholytes⁴⁸⁻⁵¹) or specific interactions (e.g., H-bonding of complementary nucleic acid base pairs⁵²⁻⁵⁶) are used to mediate hierarchical assembly. Novel hierarchical materials may also be envisioned arising from a combination of hydrophobic-mediated DEA-PEGs and specific and/or nonspecific electrostatic interactions between building blocks. With respect to what is described in this paper, the lamellar gels may be functionalized by inclusion of membrane-associated molecules (proteins, drugs); thus, creating “bioactive gels” with potential applications in molecular delivery including in therapeutics.

Experimental Section

Materials and sample preparation

The lipid DOPC (1,2-dioleoyl-*sn*-glycero-3-phosphocholine, 786.15 g/mol) was purchased from Avanti Polar Lipids. DOTAP (*N*-[1-(2,3-dioleoyloxy)propyl]-*N,N,N*-trimethylammonium methyl sulfate, 774.2 g/mol) was synthesized as described⁵⁷ with some modifications (see Supporting Information). Other chemicals were purchased from Aldrich and used as received. High-resistivity (18 M Ω cm) water was obtained from a Milli-Q Plus unit (Millipore).

The default method for sample preparation was mixing the appropriate amounts of lipid powders and water in 1.5 mL high-recovery vials (Chemglass) and incubating for the indicated time period to allow equilibration. For “water dilution” samples, a batch of sample at the indicated Φ_{water} (e.g., 50 wt% water for the DEA-PEG2K lipids and at 60 wt% water for the DEA-PEG4.6K lipids at 2.5 mol% DEA-PEG) was prepared and incubated at room temperature for 2–3 weeks for equilibration. Subsequently, appropriate amounts of this sample and water were mixed and incubated for 2 weeks. As a second, alternative method of sample preparation, appropriate weights of equilibrated samples (50 and 80 wt% water for DEA-PEG2K lipids; 60 and 90 wt% water for DEA-PEG4.6K lipids) were mixed and incubated to yield samples of intermediate water content. Samples were transferred to 1.5 mm quartz capillary tubes (Hilgenberg) and sealed with epoxy resin for X-ray scattering measurements.

Synthesis

Detailed protocols for the synthesis of the PEG-lipids and DEA-PEGs used in this work are provided in the Supporting Information.

X-ray Diffraction

Small-angle X-ray scattering (SAXS) measurements were conducted using a custom-constructed instrument in the X-ray diffraction facility of the Materials Research Laboratory at the University of California at Santa Barbara. The instrument utilizes a 50 μ m microfocus Cu-target X-ray source with a Genix parallel beam multilayer optics and monochromator system (Genix by XENOCs), a high-efficiency collimator with scatterless hybrid slits developed in-

house,⁵⁸ and a EigerR 1M solid state detector (Dectris). Data reduction and analysis were carried out using the NIKA and IRENA software packages developed at Argonne National Laboratory.^{59,60}

Results and Discussion

Synthesis

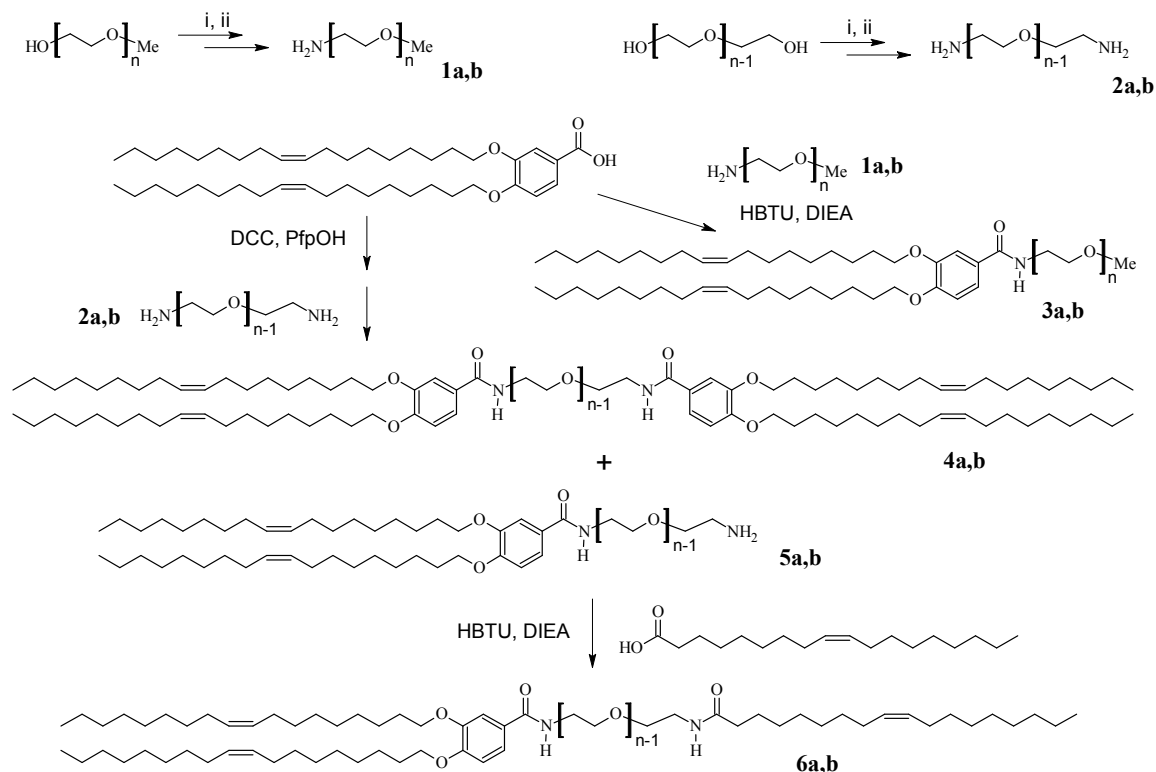
Scheme 1 shows the synthesis of the single- and double- end-anchored PEG-lipids (SEA-PEGs and DEA-PEGs) used in this work. We varied the length of the PEG tether in order to vary the range of membrane-membrane interactions, which is repulsive for SEA-PEGs and the looping conformation of DEA-PEGs, and attractive for the bridging conformation of DEA-PEGs. The hydrophobicity of the lipid end-groups was modified to look for effects of anchoring strength on the phase behavior of lamellar hydrogels, including, kinetic effects. Conversion of hydroxyl-terminated PEGs and mPEGs to the corresponding amines was readily accomplished on a multigram scale in two steps: mesylation followed by solvolysis in an excess of concentrated ammonium hydroxide solution.⁶¹ Acylation of mPEG-NH₂ (**1a,b**) with the lipid building block DOB (3,4-dioleoyloxybenzoic acid)^{48,49} yielded the control single-end-anchored PEG-lipids (**3a,b**; L-PEG) on a gram scale. Monofunctionalization of amine-terminated PEG (**2a,b**) with DOB to yield **5a,b** requires a less reactive acylation reagent and low temperature^{49,50} and yields the symmetric double-end-anchored PEG (**4a,b**; L-PEG-L) as a side product. The monofunctionalized PEG (**5a,b**) was separated by chromatography and acylated with oleic acid to yield the asymmetric double-end-anchored PEGs (**6a,b**; L-PEG-L'). Detailed synthesis procedures are provided in the Supplementary Material.

Table 1 lists the synthesized PEG-lipids with their abbreviated names, PEG molecular weight, and PEG degree of polymerization. For simplicity, we refer to the lipids with PEG molecular weights 5000 and 4600 g/mol collectively as “PEG5000-lipids”. (The difference in PEG molecular weight between the control single-end-anchored PEG-lipid and the DEA-PEGs is due to the fact that 4600 and 5000 are the readily commercially available sizes of PEG and mPEG, respectively.)

Table 1. List of the synthesized PEG-lipids with their abbreviated names, PEG molecular weight, and PEG degree of polymerization.

Compound	Notation	PEG MW	$n \approx$
3a	L-P2K	2000	45
3b	L-P5K	5000	113
4a	L-P2K-L	2000	45
4b	L-P4.6K-L	4600	104

6a	L-P2K-L'	2000	45
6b	L-P4.6K-L'	4600	104



Scheme 1. Synthesis of single- and double-end-anchored PEG-lipids; $n=45$ (PEG MW=2000 g/mol), $n=104$ (PEG MW=4600 g/mol), or $n=113$ PEG MW=5000 g/mol) Reagents and conditions: (i) methanesulfonyl chloride, Et₃N; (ii) concentrated aqueous ammonia solution; (iii) HBTU, DIEA; (iv) pentafluorophenol, DCC. DCC: dicyclohexylcarbodiimide; DIEA: diisopropylethylamine; Et₃N: triethylamine; HBTU: *N,N,N',N'*-tetramethyl-*O*-(1*H*-benzotriazol-1-yl) uronium hexafluorophosphate.

Effect of added DEA-PEG2000 on membrane spacing

To investigate the effect of added DEA-PEGs on stacks of repulsive lipid membranes, we incorporated these DEA-PEGs into membranes containing a near-equimolar mixture of neutral DOPC and univalent cationic DOTAP. We then used small-angle X-ray scattering (SAXS) to measure the interlamellar spacing at varying water content (Φ_w), between 30 wt% to 90 wt%. Membranes containing single-end-anchored PEG-lipid or no PEG-lipid served as the controls.

Figure 2 shows the X-ray scattering profiles obtained for lamellar samples containing 5 mol% of PEG2K-lipids in the membranes (panel (a) displays the control data with SEA-PEGs; panels (b-d) displays lamellar hydrogel samples with asymmetric (b) and symmetric (c,d) DEA-PEGs; panel (e) compares lamellar hydrogel samples with symmetric DEA-PEGs 1 and 2 months after preparation). At higher water content (50–60 wt% and above), the observed peaks

index to a single lamellar phase as indicated in the plots ($q_{001}:q_{002}:q_{003}=1:2:3$). The lamellar spacing $d=2\pi/q_{001}$ is the sum of the thicknesses of the membrane (lipid bilayer) and the water layer separating the membranes; that is, $d=\delta_m+\delta_w$ ($\delta_w=39$ Å for this DOTAP/DOPC composition⁶⁵.) At lower water contents, two lamellar phases are observed with the peaks of the second phase ($q_{001}:q_{002}=1:2$) at higher q , i.e., a smaller d .

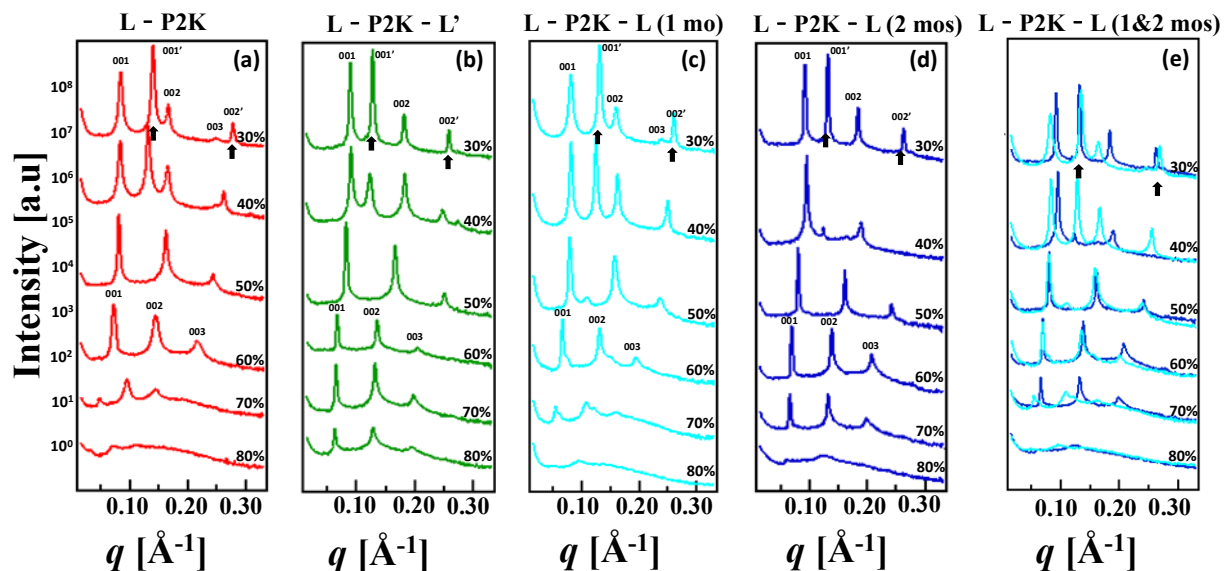


Figure 2. SAXS profiles of lyotropic phases of mixtures of DOPC, DOTAP and single- and double-end-anchored PEG2000-lipids (50/45/5 molar ratio) at varying water content (Φ_w) (30 wt% to 80 wt%). (a) Control samples containing SEA-PEG (L-P2K), one month after preparation. (b) Samples containing asymmetric DEA-PEG (L-P2K-L'), one month after preparation. (c) Samples containing symmetric DEA-PEG (L-P2K-L), one month after preparation. (d) Samples containing symmetric L-P2K-L, two months after preparation. (e) Overlay of the data shown in (c) and (d) (maintaining the color scheme; light blue: one month after preparation; dark blue: two months after preparation).

The peaks originating from the two phases observed at low water content behave very differently with increasing water content. Those at q_{001} etc. shift continuously to lower q (larger d) with increasing water content, while their intensity remains essentially constant (at water contents up to 50 wt%). In contrast, the position of the peaks at $q_{001'}$ etc. remains essentially constant as the water content increases, but their intensity decreases. A likely explanation for these observations is based on the headgroup size of the PEG-lipids: if the system formed a single phase at low water contents, the water layer between the membranes would be too thin to accommodate the PEG polymer coils without incurring a high cost in elastic energy for deforming them ($\delta_w < \delta_w^*$). Thus, a phase with a larger spacing ($\delta_w \approx \delta_w^*$; accommodating the PEG chains of the DEA-PEGs or SEA-PEGs) forms, in coexistence with a lamellar phase with a

very small spacing and very little DEA-PEG incorporated in its membranes. This is schematically illustrated in Figure 3a. As the water content increases, the phase containing the DEA-PEG is capable of incorporating more and more of the total lipid until the other phase disappears (consistent with the lever rule and the reduction of the peak height of the second phase). Consistent with this proposed mechanism, the control sample without PEG-lipid exhibits an intermediate d (between those of the two phases of PEG-lipid-containing samples) (see Figure 4).

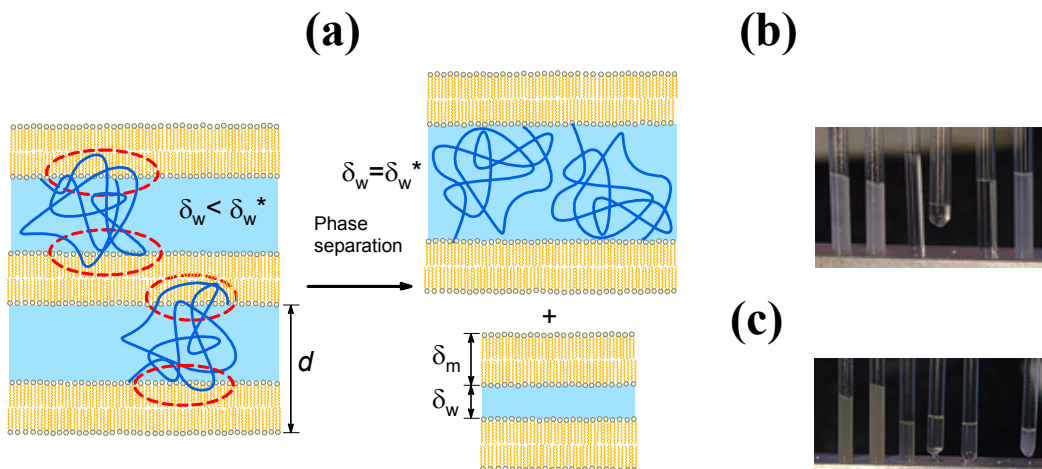


Figure 3. (a) Schematic illustration of the likely mechanism driving phase separation in PEG-lipid-containing lamellar phases at low water content. Rather than form a single phase with a water layer that is too thin ($\delta_w < \delta_w^*$) to accommodate the PEG chains without a large energy cost arising from their elastic deformation, the system phase separates into a PEG-lipid-containing phase with a larger spacing ($\delta_w = \delta_w^*$) and a phase with a thin water layer and no PEG-lipid. (b,c) Images of X-ray samples of mixtures of DOPC, DOTAP and single- and double- end-anchored PEG2000-lipids (50/45/5 molar ratio) at varying water content (Φ_w) (30, 40, 50, 60, 70, and 80 wt%, from left to right). (b) Control samples containing SEA-PEG (L-P2K). (c) Samples containing asymmetric DEA-PEG (L-P2K-L'). The opacity of the samples at high and low water content is indicative of two coexisting phases (small droplets of the minority phase suspended in the majority phase).

It is worth pointing out that, because of their charge, the interactions between the membranes are repulsive even in the absence of any PEG-lipid. (Lamellar phases of DOTAP/DOPC at a similar composition without PEG-lipids swell continuously with increasing water content up to (at least) 80 wt% water; see Figure 4.) Thus, both phases will be inclined to expand with increasing water content. The fact that only the PEG-lipid-containing phase (lower q /larger d) swells suggests that the limited amount of water that is available swells not both but only the PEG-containing phase, which must have a stronger driving force toward expansion (elastic

compression of PEG coils in addition to electrostatic repulsion) than the other phase (electrostatic repulsion only).

To allow assessing the changes in d in more detail, Figure 4 plots the interlamellar spacing d (calculated from the SAXS data) against water content for the 5 mol% DEA-PEG2K-containing samples and controls (single-end-anchored PEG2K-lipids, L-P2K, and no PEG-lipid). Comparing the behavior of the two control samples, i.e., membranes without any PEG-lipid and membranes containing single-end-anchored PEG-lipid (L-P2K), shows that while both show a continuous increase of d with water content, d is larger (in the single-lamellar-phase regime at high water content) for the samples containing PEG-lipid. In the control sample without PEG-lipid, d increases because of electrostatic repulsion, from $d=71.9$ Å ($\Phi_w=50\%$) to $d=158$ Å ($\Phi_w=80\%$). The larger interlamellar distance for the control with SEA-PEGs (e.g., $d=206.9$ Å at $\Phi_w=80$ wt%) suggests that the presence of the PEG chains results in additional repulsive interactions even at large water content. At low water content, the samples containing PEG-lipid form two phases (with d similar to the phases observed for the DEA-PEG2Ks), consistent with the rationale we proposed above. Thus, all PEG-lipid containing lamellar phases yield an increased intermembrane repulsion at lower water contents. DEA-PEG2K lipid offers both steric repulsion and attractive interaction, as it has two hydrophilic groups, so some of them can adopt the bridging conformation between two membranes, which will limit the swelling of membranes, and some the looping conformation, which is repulsive.

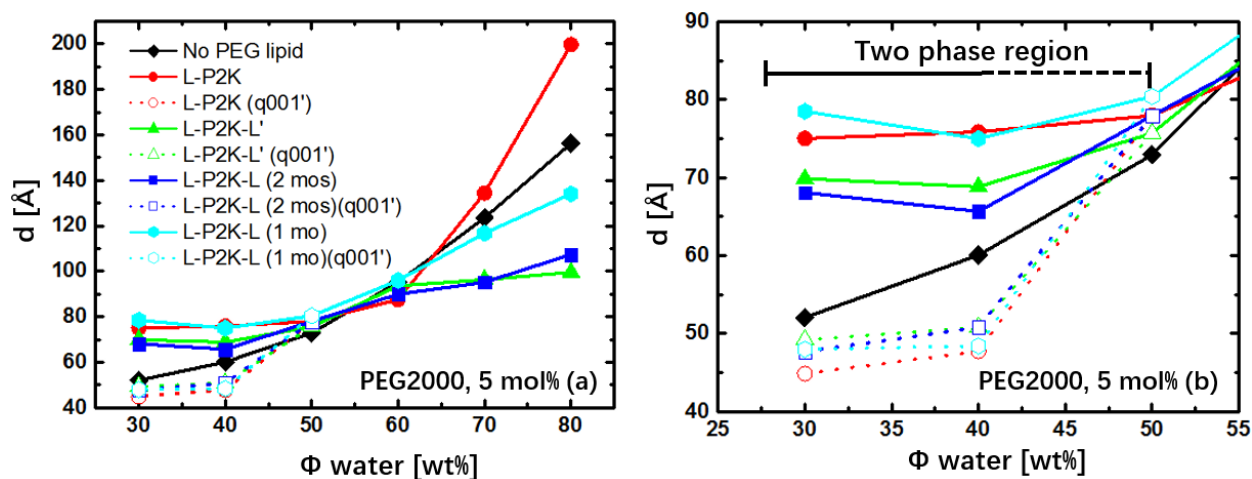


Figure 4. Evolution of the interlamellar distance d with water content for lamellar phases of membranes containing 5 mol% of double-end-anchored PEG2K-lipids and controls (single-end-anchored PEG2K-lipids and no PEG-lipid). Membrane compositions: DOTAP/DOPC/PEG2K-lipid=45/50/5 (molar ratio) or DOTAP/DOPC 1:1 (molar ratio) (control, no PEG-lipid). (a) Plot showing the entire range of water contents investigated. (b) Enlarged view of the data shown in (a) for low water content, where two lamellar phases are observed for samples containing PEG-lipids.

Focusing now on the peak positions at higher water content (≥ 50 wt%) (Figure 2), it is evident that the peaks for the control sample shift to continuously lower values of q (i.e., reflecting an interlamellar spacing that increases with water content). In contrast, the position of the first peak stays nearly constant for samples containing double-end-anchored PEG-lipids at ≥ 60 wt% water, implying that d levels off at this water content. Thus, multilayer membranes containing DEA-PEG2Ks incorporated water between $\Phi_w=50$ wt% and 60 wt% (e.g., with d increasing from 73.8 Å to 90.4 Å for L'-PEG2K-L), but did not swell much beyond $\Phi_w=60$ wt% (see Figure 4 with $d=91.8$ Å and 94.6 Å for $\Phi_w=70$ wt% and 80 wt%, respectively, for L'-PEG2K-L).

The observation of this distinct “locked state”, in which the membrane ceases to swell with further increases in water content, indicates the presence of strong attractive interactions, which limit the distance between the membranes. The likely source of these interactions is the formation of physical cross-bridges by the DEA-PEG component of the membrane, which tether opposing membranes together. The energetic cost of stretching the PEG chain then limits the distance between two membranes and only permits swelling of the lamellar phase over a small water dilution range, with d leveling off beyond a certain spacing. After this point, additional water in the sample forms a separate phase. Note that this observation shows that the lipid anchor binding energy for both the single- and double-tail anchor is sufficiently large (several $k_B T$) that phase separation (i.e., the formation of a new phase of mainly water) is favored over unbinding of the anchor from the membrane or an exclusive prevalence of the looping conformation. The phase separation at high as well as low water content also manifests in the macroscopic appearance of the samples. Samples at low water content are milky/opaque, indicative of phase separation (i.e., small droplets of the minority phase (with distinct refractive index) are suspended in the majority phase, giving rise to the milky appearance). The samples at intermediate water content are clear (indicating a single phase), and samples at high water content again are opaque with a distinct, clear and non-birefringent top phase (presumably water) (Figure 3 (c)).

Another notable feature of the data shown in Figure 2 is its time dependence. We measured the SAXS of the samples one and two months after their preparation. The scattering profiles of the samples containing L-P2K and L-P2K-L' were the same for both time points, suggesting that they had reached equilibrium by the time they were first investigated at one month. In contrast, the scattering profiles of the samples containing L-P2K-L were different for the two time points (see Figure 2, parts c-e), ceasing to change only at the two month time point. Thus, samples containing the symmetric double-end-anchored PEG2K-lipid took a longer time to reach equilibrium (see also Figure 4).

The likely explanation for this slower equilibration is found in the properties of the anchoring groups of the DEA-PEGs: L-P2K-L has a double-tail DOB group at each end of the PEG chain, while one of these is replaced by a single-tail, oleic acid moiety in L-P2K-L'. The single chain of oleic acid has a much higher solubility in water than the two long carbon chains of DOB, which increases the probability that it can be found in the intermediate state schematically shown in Figure 1B (right). This facilitates not only interconversion between the bridging and looping states, but also any rearrangements of membranes containing the L-P2K-L' DEA-PEG, thus accelerating equilibration. It is interesting to note that d decreases during equilibration: after one month, the interlamellar spacing of samples at higher water content is close to that of the control samples without PEG-lipid; after two months, it matches the lower d of the L-P2K-L'-containing samples (see Figure 4).

Effect of DEA-PEG2000 concentration and reversible transition from a locked to an unlocked (membrane unbinding) state

Having established that DEA-PEG2K lipids mediate attractive interactions between membranes, we sought to investigate the effect of the concentration of the DEA-PEGs in the membrane. Thus, we reduced the concentration of the DEA-P2K-lipids from 5 mol% to 2.5 mol%. The X-ray scattering profiles for these samples are shown in Figures S1 and S3 in the Supporting Information, while Figure 5 shows the values of d calculated from the scattering data.

The behavior at low to intermediate (70 wt%) water content is similar to that seen for the samples with higher DEA-PEG concentration (Figure 4). Two lamellar phases coexist at low water content, and a single lamellar phase is observed at intermediate water content (40 to 70 wt%). The interlamellar spacing for DEA-P2K-containing samples at 70 wt% water is much lower than that of the controls and nearly identical (at just under 10 nm) to that at 60 wt% water. However, initial exploratory measurements showed that d had increased strongly at 80 wt% of water, to a value similar to the controls (about 25 nm) (Figure S1). This unlocking of the membrane distance (i.e. membrane unbinding) suggested that the bridging interactions had been broken, and we investigated the range of 60 to 80 wt% water with a larger number of samples prepared by two different methods. For one set of samples, we added appropriate amounts of water to the lamellar phase at 50 wt% of water, to create mixtures containing from 62.5 to 80 wt% of water. For the second set of samples, we combined appropriate amounts of samples at 50 wt% (lamellar phase prior to “locking”) and 80 wt% (“unlocked” regime) to prepare a series of samples containing 60 to 77.5 wt% water. Both sets of samples yield the same peak positions and thus interlamellar spacing (Figures S3 and 5), strongly suggesting that they represent the equilibrium state, and that the “locked” regime is not a kinetically trapped state. The plot of the interlamellar spacing (Figure 5) shows that the behavior of the samples is initially similar to those containing 5 mol% DEA-P2Ks. An increase in d from 50 wt% to 60 wt% (as in the controls) is followed first by a near plateau. However, a further increase in water content leads to

a slow increase in d (with d remaining well below that of the controls) until, between 75 and 80% water, d rapidly grows. Thus, this lower concentration of DEA-P2Ks is able to “lock” the distance between membranes initially, but this attraction is weaker (as evidenced by the slight but measurable expansion) than at 5 mol% DEA-PEG and breaks down at very high water content. It is interesting to note that this behavior is independent of the anchoring groups on the DEA-PEG, despite the fact that one would expect a stronger anchoring by the double-tail anchors. It seems, however, that this is not relevant for the equilibrium state.

Intriguingly, the breakdown of the locking at high water content is readily *reversible*. This is evident both from the set of samples prepared by mixing phases with 50 and 80 wt% water and the fact that an “unlocked” sample (80 wt% water, L-P2K-L’) that lost water over time returned to the “locked” state (Figure S4). Thus, the membranes can be unlocked by adding water and relocked by either removing water or adding lamellar phase of the same lipid composition but containing less water. On a molecular level, this means that membranes with DEA-P2Ks exclusively in the looping conformation (at high water content) readily regain the bridging conformation.

Note that already after one month, the scattering profiles for symmetric and asymmetric DEA-PEGs were identical, meaning that equilibration was more rapid at this concentration of PEG-lipid in the membrane.

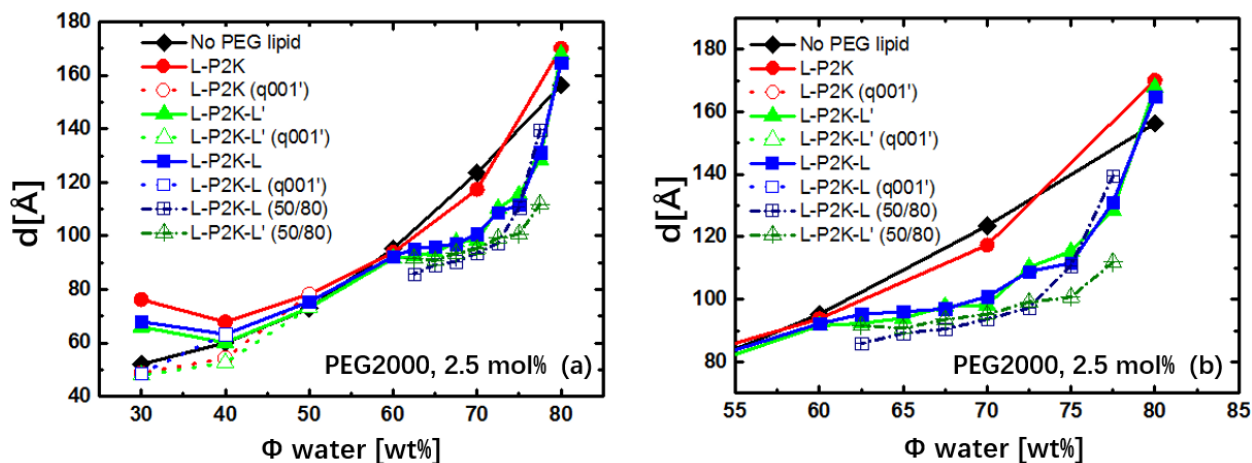


Figure 5. Evolution of the interlamellar distance d with water content (Φ_w) for lamellar phases of membranes containing 2.5 mol% of double-end-anchored PEG2K-lipids and controls (single-end-anchored PEG2K-lipids and no PEG-lipid). Membrane compositions: DOTAP/DOPC/PEG2K-lipid=50/47.5/2.5 (molar ratio) or DOTAP/DOPC 1:1 (molar ratio) (control with no PEG-lipid). The suffix “(50/80)” in the legend designates samples prepared by mixing appropriate amounts of lamellar phases with 50 and 80 wt% water. The suffix “(q001’)” in the legend indicates data for the second lamellar phase that was observed for the respective PEG-lipid (at low water content).

Effect of added DEA-PEG5000 and comparison to DEA-PEG2000

To assess the effect of PEG molecular weight, we prepared samples using the single- and double- end-anchored PEG5K-lipids (Table 1, **4b** and **6b**, as well as **3b** as the control). In these lipids, the length of the PEG chain is more than doubled compared to the PEG2K-lipids. Figure S5 in the Supporting Information shows the X-ray scattering profiles, and Figure 6 shows the calculated interlamellar spacing as a function of water content for samples containing 5 mol% of these lipids in their membranes.

At low water content, two lamellar phases are observed (as for the SEA-PEG2Ks and DEA-PEG2Ks). However, the interlamellar spacing of the phase with the larger spacing is higher (e.g., $d = 85.9$ vs 68.8 Å for L-PEG-L' at 40 wt% water) than for the PEG2K-lipids. (The spacing of the second phase is unchanged, and again lower than that of the control without PEG-lipid.) This is consistent with the interpretation we proposed above, because the larger PEG chain requires a thicker water layer and thus larger interlamellar spacing to be accommodated without a large cost in elastic energy.

From 50 to 90 wt% of water, SAXS indicates a single lamellar phase. Again, the interlamellar spacing increases continuously with water content for the controls (no PEG-lipid and single-end-anchored PEG-lipid). For the double-end-anchored PEG-lipids, however, it only increases initially between $\Phi_w=50$ wt% ($d = 95.4$ Å for L-P4K6-L') and $\Phi_w=70$ wt% ($d = 126.3$ Å for L-P4K6-L'), with d leveling off beyond that ($d = 125.5$ Å at $\Phi_w = 80$ wt% for L-P4K6-L'). Compared to the PEG2K-lipids, the leveling-off happens at higher water content (≈ 70 wt%) and (thus) higher spacing (at 80 wt% water, $d = 129.0$ (L-P4k6-L') and 133.5 Å (L-P4k6-L)). In other words, the double-end-anchored PEG4600 mediate an attractive interaction at a longer range than the PEG2000-lipids.

Samples with both symmetric and asymmetric DEA-P5K-lipids had reached equilibrium one month after sample preparation, in contrast to the DEA-P2K-lipids (where L-P2K-L required more time).

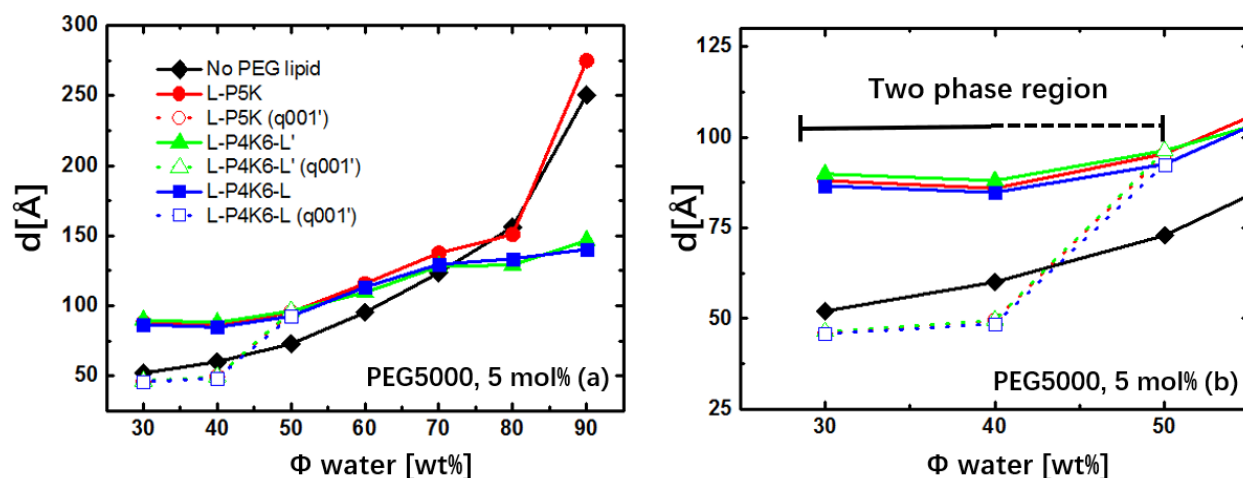


Figure 6. Evolution of the interlamellar distance d with water content for lamellar phases of membranes containing 5 mol% of double-end-anchored PEG4.6K-lipids and controls (single-end-anchored PEG5K-lipids and no PEG-lipid). Membrane compositions: DOTAP/DOPC/PEG-lipid=50/45/5 (molar ratio) or DOTAP/DOPC 1:1 (molar ratio) (control with no PEG-lipid). The suffix “(q001’)” in the legend indicates data for the second lamellar phase that was observed for the respective PEG-lipid (at low water content). (a) Plot showing the entire range of water contents investigated. (b) Enlarged view of the data shown in (a) for low water content, where two lamellar phases are observed for samples containing PEG-lipids.

We also investigated the effect of PEG-lipid concentration on the attractive interactions mediated by DEA-PEG5K, by preparing lamellar membrane samples containing only 2.5 mol% of DEA-PEG5K in the membranes. Because the studies with DEA-PEG2K showed an “unlocking” of the interlamellar spacing at high water contents (Figure 5), we prepared an increased number of samples between 70 and 90 wt% water. Again, two sets of samples were prepared; one by adding water to a concentrated lamellar phase and another by combining appropriate amounts of the two samples containing 60 and 90 wt% water, respectively. Figure 7 shows the interlamellar spacing as a function of water content for all samples. (See Figure S6 in the Supporting Information for the scattering profiles.) As before, the samples prepared in different ways showed essentially the same interlamellar spacings, strongly suggesting that the system is at equilibrium.

In contrast to the DEA-PEG2K containing samples, the phase behavior of lamellar membranes with DEA-PEG5K at 5 mol% is the same as at 2.5 mol%. In particular, locking of the interlamellar spacing occurs at the same water content (>70 wt%) and d (about 130 Å) and, importantly, the locking remains intact even at 90 wt% water. The likely reason that the locking is maintained is that the electrostatic repulsion is weaker at the longer distance at which the DEA-P5K-lipids lock the membranes, and thus this locking is easier to maintain. The fact that L-P4K6-L exhibits two lamellar phases even at 50 wt% water is most likely due to incomplete

equilibration of the sample, again showing that the asymmetric DEA-PEGs promote faster equilibration.

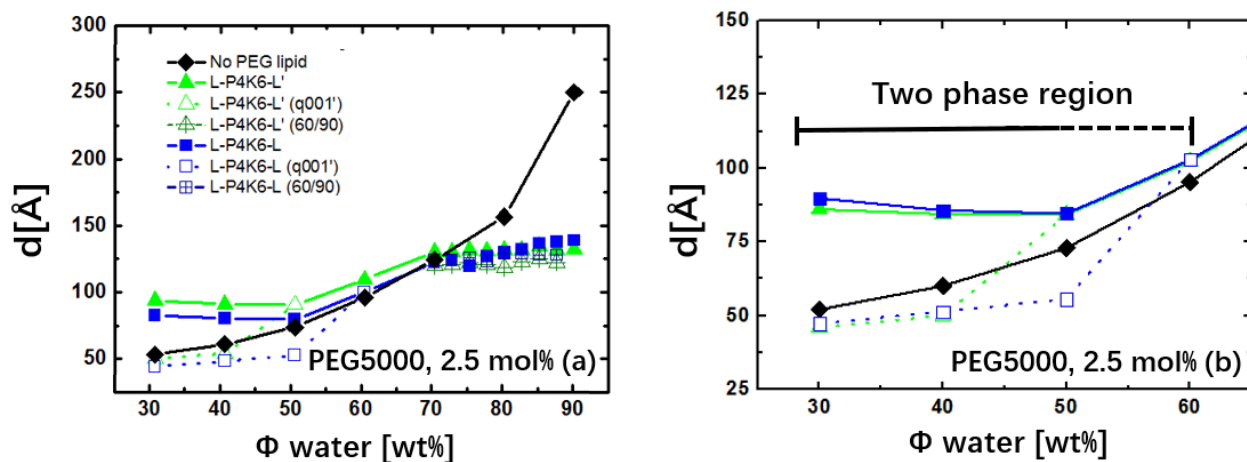


Figure 7. Evolution of the interlamellar spacing d with water content for lamellar phases containing 2.5 mol% of double-end-anchored PEG4.6K-lipids and controls (no PEG-lipid). Membrane compositions: DOTAP/DOPC/PEG-lipid=50/47.5/2.5 (molar ratio) or DOTAP/DOPC 1:1 (molar ratio) (control, no PEG-lipid). (a) Plot showing the entire range of water contents investigated. (b) Enlarged view of the data shown in (a) for low water content. The suffix “(60/90)” in the legend designates samples prepared by mixing appropriate amounts of lamellar phases with 60 and 90 wt% water. The suffix “(q001)” in the legend indicates data for the second lamellar phase that was observed for the respective PEG-lipid (at low water content).

Based on the data shown in Figures 4–7, we can quantify the dependence of the interlamellar distance d in the locked state on PEG molecular weight. Calculating the PEG radius of gyration as $R_G = a n^{3/5}$ (for a polymer in a good solvent), with $a = 3.6$ Å the monomer length and n =degree of polymerization, leads to $R_G = 35.3$ Å and 58.4 Å for PEG2K ($n = 45$) and PEG4.6K ($n = 104$), respectively. This is consistent with measured values of 35 Å and 62 Å for PEG2K and PEG5K ($n = 113$), respectively.^{8,66,67} Subtracting the membrane thickness $\delta_m = 39$ Å⁶⁵ yields an average locked water spacing between opposing membranes of $\delta_w = 56.5$ Å or 1.60 R_G and $\delta_w = 89.1$ Å or 1.53 R_G for membranes locked with DEA-PEG2Ks and PEG4.6Ks, respectively. This finding is consistent with the expectation that the maximum separation between tethered membranes should be of order R_G , because beyond that the elastic cost of PEG chain stretching ($\approx k_B T (\delta_w / R_G)^2$) would rapidly exceed the available thermal energy $k_B T$. However, the locking distance is less than the physical size of the PEG chain of the tether ($= 2R_{\text{physical}} = 2(5/3)^{1/2} R_G$), which indicates that end-anchored PEG between the layers is considerably more compressed compared to free PEG. To rationalize this, one must take into account that the conformational space of the PEG chain of the DEA-PEG is reduced by the confinement of the end groups to the

membrane surface. The remarkably simple relation, $\delta_w \approx 1.6 R_G = 1.6 a n^{3/5}$, between the tethering distance and the length of the PEG tether allows control of the wall-to-wall spacing between opposing membranes by varying the molecular weight (MW) of the PEG tether. A plot of the interlamellar spacing combining the data for the DEA-PEGs for PEG2000- and PEG5000-tethers demonstrates this finding (see Figure S7 in the Supporting Information). Note that the arguments above all refer to the regime of high water content, where the DEA-PEG mediates attractive interactions. At low water content, the PEG chains also mediate repulsive interactions (see above in the discussion of Figure 3). In this regime, the PEG lipid forces a certain minimum δ_w^* (in the phase containing the PEG-lipid) due to (repulsive) excluded volume interaction of polymer chains confined between opposing surfaces. Consistent with theoretical considerations and related experimental results for supported lipid bilayers,^{68,69} this distance δ_w^* is of order R_G , increasing with molecular weight of the PEG chain.

A more complete theoretical understanding of the observed phenomena is beyond the scope of this paper because besides the lipid anchor binding energy and the elastic energy of stretching, such theory must also consider the repulsive electrostatic force between the membranes (which is balanced by the elastic energy of stretching) and the free energy of phase separation (which occurs both at low water content (two lipid-containing phases) and high water content (a lipid-containing phase and water)). Only thus considering the whole system rather an individual DEA-PEG molecule will enable a theoretical understanding of why, e.g., the preservation of “locking”, does not only require a lipid anchor binding energy larger than several $k_B T$ (which is the case for both single- and double-tail anchors) but also a sufficient concentration of the DEA-PEG in the membrane (see the “unlocking” for DEA-PEG2000 at 2.5 mol%).

Conclusions

We have demonstrated that double-end-anchored PEG-lipids can reversibly control the interlayer spacing in a lamellar hydrogel of charged swellable membranes, locking the membrane wall-to-wall distance limiting the amount of water that is incorporated into the lamellar phase at higher water content. This is due to the bridging conformation dominating over the looping conformation of DEA-PEGs. The locking distance is set by the competition between attractive (due to bridging) and repulsive (due to looping and interlayer electrostatic) interactions and follows a predictable relation to the radius of gyration (i.e., the molecular weight) of the PEG chain as $d \approx 1.6 R_G$. Meanwhile, the strength of locking/tethering interaction may be tuned by varying the concentration of DEA-PEG in the membrane. Notably, in the case of DEA-PEG2K at low concentration (2.5 mol%), the lamellar hydrogel may be designed to reversibly switch between the locked (constant spacing with increased addition of water) and unlocked (membrane unbinding) states.

Thus, DEA-PEGs are capable of complementing the protective abilities of PEG-lipids (which are based on repulsive steric interactions) by adding attractive interactions with a tunable length scale (via the length of the PEG chain) between membranes. We anticipate applications of this concept that will harness hydrophobic interactions for hierarchical assembly of lipid- or surfactant-coated building blocks with distinct shape and size in a manner similar to, but orthogonal to and complementary with the electrostatic or base pairing interactions that have been used extensively in the literature. Of possibly enabling importance for applications is that the structure of the anchoring group controls the kinetics of forming the locked phase. The newly designed DEA-PEGs with a single hydrophobic chain on one end (L-PEG-L'; Table 1 **6a,b**) lead to faster equilibration than those with two double-chain anchors.

One area for applications is the development of tunable biomaterial interfaces for delivery of macromolecules (e.g., DNA) by mediating nonspecific but charge-independent attractive (tethering) interactions with target membrane compartments. This is inspired by retroviruses, which already employ this concept: their transmembrane protein contains a protruding external domain consisting of a hydrophilic protein segment followed by a shorter hydrophobic segment at the N-terminus. This hydrophobic segment is designed to insert into the host plasma membrane, effectively tethering the virus to the host. The tethering is followed by the initiation of fusion of the envelope and cell plasma membranes, which involves fusogenic membrane-associated proteins.⁷⁰⁻⁷² We plan to use DEA-PEGs a similar manner to facilitate fusion of cationic liposome–DNA complexes with endosomal membranes, to overcome the crucial barrier of endosomal escape.

Further future work will explore additional methods of tuning membrane interactions and reversibly switching between the locked and unlocked states (looping and bridging conformations), such as varying the membrane charge density, chemically (and reversibly) switching between single- and double-end-anchored PEG-lipids, and developing additional means of adding competing repulsion. Another avenue for future research is varying the anchoring end groups of DEA-PEGs, for example in ways that allow tethering of other (not membrane-coated) building blocks.

Acknowledgments

This work was supported by the US Department of Energy (DOE), Office of Basic Energy Sciences, Division of Materials Sciences and Engineering under award number DE-FG02-06ER46314 (self- and directed assembly in charged biomolecular materials systems). Partial support was further provided by the US National Science Foundation (NSF) under award number DMR-1807327 (membrane phase behavior) and the by the US National Institute of Health under award Number R01GM130769 (synthesis of double-end-anchored-PEGs for tethering of vesicles). E.W. was supported in part by the National Science Foundation Graduate Research

Fellowship under Grant No. DGE 1144085. W.Q. acknowledges support from the International Science & Technology Cooperation Program of China (No. 2015DFA41670). The research reported here made use of shared experimental facilities of the Materials Research Laboratory at UCSB: an NSF MRSEC (supported by NSF DMR 1720256) and a member of the NSF-supported Materials Research Facilities Network (www.mrfn.org).

Supporting Information.

Detailed synthesis procedures, equations used to calculate sample compositions, additional SAXS profiles and plots of d vs Φ_{water} (as detailed in the text).

References

1. Fratzl, P.; Speck, T.; Gorb, S.: Function by Internal Structure. *Bioinspiration Biomimetics* **2016**, *11*, 060301.
2. Mishnaevsky, L.; Tsapatsis, M.: Hierarchical Materials: Background and Perspectives. *MRS Bull.* **2016**, *41*, 661-664. DOI: 10.1557/mrs.2016.189.
3. Lakes, R.: Materials with Structural Hierarchy. *Nature* **1993**, *361*, 511. DOI: 10.1038/361511a0.
4. Fratzl, P.; Weinkamer, R.: Nature's Hierarchical Materials. *Prog. Mater. Sci.* **2007**, *52*, 1263-1334. DOI: 10.1016/j.pmatsci.2007.06.001.
5. Nel, A. E.; Madler, L.; Velegol, D.; Xia, T.; Hoek, E. M. V.; Somasundaran, P.; Klaessig, F.; Castranova, V.; Thompson, M.: Understanding Biophysicochemical Interactions at the Nano-Bio Interface. *Nat. Mater.* **2009**, *8*, 543-557. DOI: 10.1038/nmat2442.
6. Xia, F.; Jiang, L.: Bio-Inspired, Smart, Multiscale Interfacial Materials. *Adv. Mater.* **2008**, *20*, 2842-2858. DOI: 10.1002/adma.200800836.
7. Lee, H.; Dellatore, S. M.; Miller, W. M.; Messersmith, P. B.: Mussel-Inspired Surface Chemistry for Multifunctional Coatings. *Science* **2007**, *318*, 426-430. DOI: 10.1126/science.1147241.
8. Kuhl, T. L.; Leckband, D. E.; Lasic, D. D.; Israelachvili, J. N.: Modulation of Interaction Forces Between Bilayers Exposing Short-Chained Ethylene Oxide Headgroups. *Biophys. J.* **1994**, *66*, 1479-1488. DOI: 10.1016/S0006-3495(94)80938-5.
9. Torchilin, V. P.: How do Polymers Prolong Circulation Time of Liposomes? *J. Liposome Res.* **1996**, *6*, 99-116. DOI: 10.3109/08982109609037204.
10. Gabizon, A.; Papahadjopoulos, D.: Liposome Formulations with Prolonged Circulation Time in Blood and Enhanced Uptake by Tumors. *Proc. Natl. Acad. Sci. U. S. A.* **1988**, *85*, 6949-6953. DOI: 10.1073/pnas.85.18.6949.
11. Allen, T. M.; Hansen, C.; Rutledge, J.: Liposomes with Prolonged Circulation Times: Factors Affecting Uptake by Reticuloendothelial and Other Tissues. *Biochim. Biophys. Acta, Biomembr.* **1989**, *981*, 27-35. DOI: 10.1016/0005-2736(89)90078-3.
12. Lasic, D. D.; Martin, F., Eds.: *Stealth Liposomes*. CRC Press: Boca Raton, **1995**.
13. Lasic, D. D.; Needham, D.: The "Stealth" Liposome: A Prototypical Biomaterial. *Chem. Rev.* **1995**, *95*, 2601-2628. DOI: 10.1021/cr00040a001.

14. Allen, T. M.: Long-circulating (Sterically Stabilized) Liposomes for Targeted Drug Delivery. *Trends Pharmacol. Sci.* **1994**, *15*, 215-220. DOI: 10.1016/0165-6147(94)90314-X.
15. Woodle, M. C.: Sterically Stabilized Liposome Therapeutics. *Adv. Drug Deliv. Rev.* **1995**, *16*, 249-265. DOI: 10.1016/0169-409X(95)00028-6.
16. Immordino, M. L.; Dosio, F.; Cattel, L.: Stealth liposomes: Review of the Basic Science, Rationale, and Clinical Applications, Existing and Potential. *Int. J. Nanomed.* **2006**, *1*, 297-315.
17. Eloy, J. O.; Petrilli, R.; Trevizan, L. N. F.; Chorilli, M.: Immunoliposomes: A Review on Functionalization Strategies and Targets for Drug Delivery. *Colloids Surf., B* **2017**, *159*, 454-467. DOI: 10.1016/j.colsurfb.2017.07.085.
18. Torchilin, V. P.: Multifunctional, Stimuli-Sensitive Nanoparticulate Systems for Drug Delivery. *Nat. Rev. Drug Discovery* **2014**, *13*, 813-827. DOI: 10.1038/nrd4333.
19. Zalipsky, S.; Puntambekar, B.; Boulikas, P.; Engbers, C. M.; Woodle, M. C.: Peptide Attachment to Extremities of Liposomal Surface Grafted PEG Chains: Preparation of the Long-Circulating Form of Laminin Pentapeptide, YIGSR. *Bioconjugate Chem.* **1995**, *6*, 705-708. DOI: 10.1021/bc00036a008.
20. Lee, R. J.; Low, P. S.: Delivery of Liposomes into Cultured KB Cells via Folate Receptor-Mediated Endocytosis. *J. Biol. Chem.* **1994**, *269*, 3198-3204.
21. Sudimack, J.; Lee, R. J.: Targeted Drug Delivery Via the Folate Receptor. *Adv. Drug Deliv. Rev.* **2000**, *41*, 147-162. DOI: [https://doi.org/10.1016/S0169-409X\(99\)00062-9](https://doi.org/10.1016/S0169-409X(99)00062-9).
22. Kibria, G.; Hatakeyama, H.; Ohga, N.; Hida, K.; Harashima, H.: Dual-Ligand Modification of PEGylated Liposomes Shows Better Cell Selectivity and Efficient Gene Delivery. *J. Controlled Release* **2011**, *153*, 141-148. DOI: 10.1016/j.jconrel.2011.03.012.
23. Majzoub, R. N.; Chan, C.-L.; Ewert, K. K.; Silva, B. F. B.; Liang, K. S.; Jacovetty, E. L.; Carragher, B.; Potter, C. S.; Safinya, C. R.: Uptake and Transfection Efficiency of PEGylated Cationic Liposome–DNA Complexes With and Without RGD-Tagging. *Biomaterials* **2014**, *35*, 4996-5005. DOI: 10.1016/j.biomaterials.2014.03.007.
24. Ewert, K. K.; Kotamraju, V. R.; Majzoub, R. N.; Steffes, V. M.; Wonder, E. A.; Teesalu, T.; Ruoslahti, E.; Safinya, C. R.: Synthesis of Linear and Cyclic Peptide–PEG–Lipids for Stabilization and Targeting of Cationic Liposome–DNA Complexes. *Bioorg. Med. Chem. Lett.* **2016**, *26*, 1618-1623. DOI: 10.1016/j.bmcl.2016.01.079.
25. Lipowsky, R.: Adhesion of Membranes via Anchored Stickers. *Phys. Rev. Lett.* **1996**, *77*, 1652-1655. DOI: 10.1103/PhysRevLett.77.1652.
26. Lipowsky, R.: Flexible Membranes with Anchored Polymers. *Colloids Surf. A* **1997**, *128*, 255-264. DOI: 10.1016/S0927-7757(96)03906-4.
27. Warriner, H. E.; Keller, S. L.; Idziak, S. H. J.; Slack, N. L.; Davidson, P.; Zasadzinski, J. A.; Safinya, C. R.: The Influence of Polymer Molecular Weight in Lamellar Gels Based on PEG-Lipids. *Biophys. J.* **1998**, *75*, 272-293. DOI: 10.1016/S0006-3495(98)77514-9.
28. Slack, N. L.; Davidson, P.; Chibbaro, M. A.; Jeppesen, C.; Eiselt, P.; Warriner, H. E.; Schmidt, H. W.; Pincus, P.; Safinya, C. R.: The Bridging Conformations of Double-End Anchored Polymer-Surfactants Destabilize a Hydrogel of Lipid Membranes. *J. Chem. Phys.* **2001**, *115*, 6252-6257. DOI: 10.1063/1.1399061.

29. Warriner, H. E.; Idziak, S. H. J.; Slack, N. L.; Davidson, P.; Safinya, C. R.: Lamellar Biogels: Fluid-Membrane-Based Hydrogels Containing Polymer Lipids. *Science* **1996**, *271*, 969-973. DOI: 10.1126/science.271.5251.969.
30. Warriner, H. E.; Davidson, P.; Slack, N. L.; Schellhorn, M.; Eiselt, P.; Idziak, S. H. J.; Schmidt, H. W.; Safinya, C. R.: Lamellar Biogels Comprising Fluid Membranes with a Newly Synthesized Class of Polyethylene Glycol-Surfactants. *J. Chem. Phys.* **1997**, *107*, 3707-3722. DOI: 10.1063/1.474726.
31. Slack, N. L.; Schellhorn, M.; Eiselt, P.; Chibbaro, M. A.; Schulze, U.; Warriner, H. E.; Davidson, P.; Schmidt, H. W.; Safinya, C. R.: Synthesis and Phase Behavior of New Amphiphilic PEG-Based Triblock Copolymers as Gelling Agents for Lamellar Liquid Crystalline Phases. *Macromolecules* **1998**, *31*, 8503-8508. DOI: 10.1021/ma980901g.
32. Keller, S. L.; Warriner, H. E.; Safinya, C. R.; Zasadzinski, J. A.: Direct Observation of a Defect-mediated Viscoelastic Transition in a Hydrogel of Lipid Membranes and Polymer Lipids. *Phys. Rev. Lett.* **1997**, *78*, 4781-4784. DOI: 10.1103/PhysRevLett.78.4781.
33. Riste, T.; Sherrington, D.: *Physics of Biomaterials: Fluctuations, Selfassembly and Evolution*. Springer Netherlands: **2012**.
34. Peppas, N. A.; Bures, P.; Leobandung, W.; Ichikawa, H.: Hydrogels in Pharmaceutical Formulations. *Eur. J. Pharm. Biopharm.* **2000**, *50*, 27-46. DOI: 10.1016/S0939-6411(00)00090-4.
35. Peppas, N. A.: *Hydrogels in Medicine and Pharmacy. Vol. 1, Fundamentals*. CRC Press: **1986**.
36. Rosiak, J. M.; Yoshii, F.: Hydrogels and Their Medical Applications. *Nucl. Instrum. Methods Phys. Res., Sect. B* **1999**, *151*, 56-64. DOI: 10.1016/S0168-583X(99)00118-4.
37. Majmudar, A. Multipurpose Hydrogel Compositions and Products. US8268345B2, 2008.
38. Pal, K.; Banthia, A. K.; Majumdar, D. K.: Polymeric Hydrogels: Characterization and Biomedical Applications. *Des. Monomers Polym.* **2009**, *12*, 197-220. DOI: 10.1163/156855509x436030.
39. Klouda, L.; Mikos, A. G.: Thermoresponsive Hydrogels in Biomedical Applications. *Eur. J. Pharm. Biopharm.* **2008**, *68*, 34-45. DOI: 10.1016/j.ejpb.2007.02.025.
40. Klouda, L.: Thermoresponsive Hydrogels in Biomedical Applications: A Seven-Year Update. *Eur. J. Pharm. Biopharm.* **2015**, *97*, 338-349. DOI: 10.1016/j.ejpb.2015.05.017.
41. Barbucci, R.: *Hydrogels. Biological Properties and Applications*. Springer: Berlin, **2009**.
42. Stein, D. B.: *Handbook of Hydrogels: Properties, Preparation & Applications*. Nova Science Publishers: New York, **2009**.
43. Kamath, K. R.; Park, K.: Biodegradable Hydrogels in Drug Delivery. *Adv. Drug Deliv. Rev.* **1993**, *11*, 59-84. DOI: 10.1016/0169-409X(93)90027-2.
44. Hoffman, A. S.: Hydrogels for Biomedical Applications. *Adv. Drug Deliv. Rev.* **2012**, *64*, 18-23. DOI: 10.1016/j.addr.2012.09.010.
45. Bouten, P. J. M.; Zonjee, M.; Bender, J.; Yauw, S. T. K.; van Goor, H.; van Hest, J. C. M.; Hoogenboom, R.: The chemistry of Tissue Adhesive Materials. *Prog. Polym. Sci.* **2014**, *39*, 1375-1405. DOI: 10.1016/j.progpolymsci.2014.02.001.
46. Rimmer, S.: *Biomedical Hydrogels: Biochemistry, Manufacture and Medical Applications*. Elsevier: **2011**.
47. Hannun, Y. A.; Obeid, L. M.: Principles of Bioactive Lipid Signalling: Lessons from Sphingolipids. *Nat. Rev. Mol. Cell Biol.* **2008**, *9*, 139. DOI: 10.1038/nrm2329.

48. Chung, P. J.; Song, C.; Deek, J.; Miller, H. P.; Li, Y.; Choi, M. C.; Wilson, L.; Feinstein, S. C.; Safinya, C. R.: Tau Mediates Microtubule Bundle Architectures Mimicking Fascicles of Microtubules Found in the Axon Initial Segment. *Nature Comm.* **2016**, *7*, 12278. DOI: [10.1038/ncomms12278](https://doi.org/10.1038/ncomms12278).
49. Safinya, C. R.; Chung, P. J.; Song, C.; Li, Y.; Ewert, K. K.; Choi, M. C.: The Effect of Multivalent Cations and Tau on Paclitaxel-Stabilized Microtubule Assembly, Disassembly, and Structure. *Adv. Colloid Interf. Sci.* **2016**, *232*, 9-16. DOI: [10.1016/j.cis.2015.11.002](https://doi.org/10.1016/j.cis.2015.11.002)
50. Deek, J.; Chung, P. J.; Kayser, J.; Bausch, A. R.; Safinya, C. R.: Neurofilament Sidearms Modulate Parallel and Crossed-Filament Orientations Inducing Nematic to Isotropic and Re-Entrant Birefringent Hydrogels. *Nature Comm.* **2013**, *4*, 2224. DOI: [10.1038/ncomms3224](https://doi.org/10.1038/ncomms3224).
51. Beck, R.; Deek, J.; Jones, J. B.; Safinya, C. R.: Gel Expanded-Gel Condensed Transition in Neurofilament Networks Revealed by Direct Force Measurements. *Nature Mat.* **2010**, *9*, 40-46.
52. Mirkin, C. A.; Letsinger, R. L.; Mucic, R. C.; Stohrhoff, J. J.: A DNA-Based Method for Rationally Assembling Nanoparticles into Macroscopic Materials. *Nature* **1996**, *382*, 607–609.
53. Elghanian, R.; Stohrhoff, J. J.; Mucic, R. C.; Letsinger, R. L.; Mirkin, C. A.: Selective Colorimetric Detection of Polynucleotides Based on the Distance-Dependent Optical Properties of Gold Nanoparticles. *Science* **1997**, *277*, 1078–1081.
54. Nykypanchuk, D.; Maye, M. M.; van der Lelie, D.; Gang, O.: DNA-Guided Crystallization of Colloidal Nanoparticles. *Nature* **2008**, *451*, 549–552.
55. Maye, M. M.; Nykypanchuk, D.; van der Lelie, D.; Gang, O.: A Simple Method for Kinetic Control of DNA-Induced Nanoparticle Assembly. *J. Am. Chem. Soc.* **2006**, *128*, 14020–14021.
56. Seeman, N. C.: DNA in a Sorld *Nature* **2003**, *421*, 427–431.
57. Massing, U.; Kley, J. T.; Gürtesch, L.; Fankhaenel, S.: A Simple Approach to DOTAP and Its Analogs Bearing Different Fatty Acids. *Chem. Phys. Lipids* **2000**, *105*, 189-191. DOI: [10.1016/S0009-3084\(00\)00121-3](https://doi.org/10.1016/S0009-3084(00)00121-3).
58. Li, Y.; Beck, R.; Huang, T.; Choi, M. C.; Divinagracia, M.: Scatterless Hybrid Metal-Single-Crystal Slit for Small-Angle X-ray Scattering and High-Resolution X-ray Diffraction. *J. Appl. Crystallogr.* **2008**, *41*, 1134-1139. DOI: [10.1107/S0021889808031129](https://doi.org/10.1107/S0021889808031129).
59. Ilavsky, J.: Nika: Software for Two-Dimensional Data Reduction. *J. Appl. Crystallogr.* **2012**, *45*, 324-328. DOI: [10.1107/S0021889812004037](https://doi.org/10.1107/S0021889812004037).
60. Ilavsky, J.; Jemian, P. R.: Irena: Tool Suite for Modeling and Analysis of Small-Angle Scattering. *J. Appl. Crystallogr.* **2009**, *42*, 347-353. DOI: [10.1107/S0021889809002222](https://doi.org/10.1107/S0021889809002222).
61. Aronov, O.; Horowitz, A. T.; Gabizon, A.; Gibson, D.: Folate-Targeted PEG as a Potential Carrier for Carboplatin Analogs. Synthesis and in Vitro Studies. *Bioconjugate Chem.* **2003**, *14*, 563-574. DOI: [10.1021/bc025642l](https://doi.org/10.1021/bc025642l).
62. Schulze, U.; Schmidt, H. W.; Safinya, C. R.: Synthesis of Novel Cationic Poly(Ethylene Glycol) Containing Lipids. *Bioconjugate Chem.* **1999**, *10*, 548-552. DOI: [10.1021/bc9801068](https://doi.org/10.1021/bc9801068).
63. Ewert, K. K.; Kotamraju, V. R.; Majzoub, R. N.; Steffes, V. M.; Wonder, E. A.; Teesalu, T.; Ruoslahti, E.; Safinya, C. R.: Synthesis of Linear and Cyclic Peptide–PEG–lipids for Stabilization and Targeting of Cationic Liposome–DNA complexes. *Bioorg. Med. Chem. Lett.* **2016**, *26*, 1618-1623. DOI: [10.1016/j.bmcl.2016.01.079](https://doi.org/10.1016/j.bmcl.2016.01.079).

64. Jacobson, A. R.; Makris, A. N.; Sayre, L. M.: Monoacylation of Symmetrical Diamines. *J. Org. Chem.* **1987**, *52*, 2592-2594. DOI: 10.1021/jo00388a048.
65. Rädler, J. O.; Koltover, I.; Salditt, T.; Safinya, C. R.: Structure of DNA-Cationic Liposome Complexes: DNA Intercalation in Multilamellar Membranes in Distinct Interhelical Packing Regimes. *Science* **1997**, *275*, 810-814. DOI: 10.1126/science.275.5301.810.
66. Needham, D.; McIntosh, T. J.; Lasic, D. D.: Repulsive Interactions and Mechanical Stability of Polymer-Grafted Lipid Membranes. *Biochim. Biophys. Acta, Biomembr.* **1992**, *1108*, 40-48. DOI: 10.1016/0005-2736(92)90112-Y.
67. Kenworthy, A. K.; Hristova, K.; Needham, D.; McIntosh, T. J.: Range and magnitude of the Steric Pressure Between Bilayers Containing Phospholipids with Covalently Attached Poly(Ethylene Glycol). *Biophys. J.* **1995**, *68*, 1921-1936. DOI: 10.1016/S0006-3495(95)80369-3.
68. Watkins, E. B.; El-khoury, R. J.; Miller, C. E.; Seaby, B. G.; Majewski, J.; Marques, C. M.; Kuhl, T. L.: Structure and Thermodynamics of Lipid Bilayers on Polyethylene Glycol Cushions: Fact and Fiction of PEG Cushioned Membranes. *Langmuir* **2011**, *27*, 13618-13628. DOI: 10.1021/la200622e.
69. Daniel, C.; Sohn, K. E.; Mates, T. E.; Kramer, E. J.; Rädler, J. O.; Sackmann, E.; Nickel, B.; Andruzzi, L.: Structural Characterization of an Elevated Lipid Bilayer Obtained by Stepwise Functionalization of a Self-Assembled Alkenyl Silane Film. *Biointerphases* **2007**, *2*, 109-118. DOI: 10.1116/1.2790852.
70. Fields, B. N.; Knipe, D. M.; Howley, P. M., Eds.: *Fundamental Virology*. 3 ed.; Lippincott Williams & Wilkins: New York, **1996**.
71. Gallaher, W. R.: Detection of a Fusion Peptide Sequence in the Transmembrane Protein of Human Immunodeficiency Virus. *Cell* **1987**, *50*, 327-328. DOI: 10.1016/0092-8674(87)90485-5.
72. Freed, E. O.; Myers, D. J.; Risser, R.: Characterization of the Fusion Domain of the Human Immunodeficiency Virus Type 1 Envelope Glycoprotein gp41. *Proc. Natl. Acad. Sci. U. S. A.* **1990**, *87*, 4650-4654. DOI: 10.1073/pnas.87.12.4650.